

Learning an Astronomical Catalog of the Visible Universe through Scalable Bayesian Inference

Jeffrey Regier*, Kiran Pamnany[†], Ryan Giordano[‡], Rollin Thomas[¶], David Schlegel[§], Jon McAuliffe[‡] and Prabhat[¶]

**Department of Electrical Engineering and Computer Science, University of California, Berkeley*

†Parallel Computing Lab, Intel Corporation

‡Department of Statistics, University of California, Berkeley

§Physics Division, Lawrence Berkeley National Laboratory

¶NERSC, Lawrence Berkeley National Laboratory

Abstract—Celeste is a procedure for inferring astronomical catalogs that attains state-of-the-art scientific results. To date, Celeste has been scaled to at most hundreds of megabytes of astronomical images: Bayesian posterior inference is notoriously demanding computationally. In this paper, we report on a scalable, parallel version of Celeste, suitable for learning catalogs from modern large-scale astronomical datasets. Our algorithmic innovations include a fast numerical optimization routine for Bayesian posterior inference and a statistically efficient scheme for decomposing astronomical optimization problems into subproblems.

Our scalable implementation is written entirely in Julia, a new high-level dynamic programming language designed for scientific and numerical computing. We use Julia’s high-level constructs for shared and distributed memory parallelism, and demonstrate effective load balancing and efficient scaling on up to 8192 Xeon cores on the NERSC Cori supercomputer.

Keywords-Astronomy, Bayesian, Variational Inference, Julia, Big Data Analytics, High Performance Computing

I. INTRODUCTION

The principal product of an astronomical imaging survey is a catalog of celestial objects, such as stars and galaxies. These catalogs are generated by identifying light sources in survey images and characterizing each according to physical parameters such as brightness, color, and morphology. Astronomical catalogs are the starting point for many scientific analyses, such as theoretical modeling of individual light sources, modeling groups of similar light sources, or modeling the spatial distribution of galaxies. Catalogs also inform the design and operation of subsequent surveys using more advanced or specialized instrumentation (e.g., spectrographs). Astronomical catalogs are key tools for studying the life-cycles of stars and galaxies as well as the origin and evolution of the Universe itself.

Modern astronomical surveys produce vast amounts of complex data. The Large Synoptic Survey Telescope (LSST) is slated to capture more than 15 terabytes of new images on a daily basis [1]; overall the instrument will produce 10s–100s of PBs over the lifetime of the project. Constructing a catalog is computationally demanding for any method because of the scale of the data. Approaches to date are

largely based on computationally efficient heuristics [2], [3]. Constructing a high-quality catalog based on a rigorous statistical treatment of the problem is computationally challenging even for datasets of modest size.

Bayesian posterior inference is effective for learning astronomical catalogs because Bayesian models can combine prior knowledge of astrophysics with new data from surveys in a statistically efficient manner. Bayesian inference also yields accurate estimates of uncertainty. Because most light sources will be near the detection limit, uncertainty estimates are as important as the parameter estimates themselves for many analyses. For example, they enable robust population-level analysis even when every individual light source is highly ambiguous [4].

Celeste [5] is a procedure for inferring an astronomical catalog from a collection of images, based on a principled statistical model, that attains state-of-the-art results. While exact posterior inference is computationally intractable, the approximation proposed in [5] is nearly linear time in all relevant quantities: the number of light sources, the number of pixels, and the number of parameters. Nonetheless, it is a computationally expensive procedure, never before scaled beyond several hundreds of MBs of imaging data. The procedure described in [5] is single-threaded.

In this paper, we present a new, parallel version of Celeste that enables scaling the procedure to large datasets on large clusters. Our contributions include:

- A fast numerical optimization routine for Bayesian posterior inference.
- A statistically efficient scheme for decomposing astronomical optimization problems into sub-problems.
- A demonstration of the viability of using the high-level Julia programming language to implement a complex, real-world data analytics application on a contemporary HPC platform.
- Development and optimization of a Julia package to enable multi-node distributed memory parallelism.

II. RELATED WORK

To date, astronomical catalogs have been constructed primarily by heuristics—algorithms that may be intuitively reasonable, but that do not follow from a statistical model of the data. For the dataset we analyze in this work, discussed in Section IV, the state-of-the-art software pipeline is a heuristic called “Photo” [3]. Heuristics have a number of shortcomings. First, they typically cannot make effective use of prior information, because it is unclear how to “weight” it in relation to new information from the survey. Yet much is known about stars’ and galaxies’ colors, brightness, and shapes before new data is collected—both from previous surveys and from astrophysical theory.

Second, heuristics do not effectively combine knowledge from multiple image surveys, or even from multiple overlapping images from the same survey. They may “co-add” the overlapping images, but this effectively discards properties unique to each image, like the atmospheric conditions at the time of exposure, or the exact alignment of the pixels.

Third, heuristics do not correctly quantify uncertainty of their estimates. They may flag some estimates as particularly unreliable. But confidence intervals follow only from a statistical model. Without modeling the arrival of photons as a Poisson process, for example, there is little basis for reasoning about uncertainty in the underlying brightness of objects.

These shortcomings are addressed by the Bayesian formalism. Unknown quantities, such as the catalog entries for our problem, are modeled as unobserved random variables with prior distributions. Then the posterior distribution, that is, the conditional distribution of the latent variables given the data, encapsulates knowledge about the latent variables. Unfortunately, exact Bayesian posterior inference is computationally intractable for all but the simplest statistical models.

In Tractor [6], rather than inferring the posterior, the mode of the posterior is learned through maximum a posterior (MAP) estimation. Though MAP estimation is scalable, and retains many of the advantages of Bayesian modeling, it does not provide uncertainties, as one would obtain from posterior inference.

Approximate posterior inference is an alternative to MAP estimation and an alternative to heuristics. Markov Chain Monte Carlo (MCMC) is the most common approach to approximate posterior inference. At each iteration, MCMC draws a sample from an approximation to the posterior distribution. Unfortunately, consecutive samples are not independent. MCMC can require tens of thousands of samples to approximate the posterior. Thus, to date MCMC has only been used to infer properties of small collections of stellar and galactic images relative to the sizes of modern astronomical datasets [7]. Moreover, even given tens of thousands of MCMC samples, it is generally unknown whether

enough samples have been collected to adequately represent the posterior—the number of samples needed could, for example, grow exponentially in some dimension of the model.

Variational inference (VI) is an alternative to MCMC that uses numerical optimization to find a distribution that approximates the posterior without sampling [8]. In practice, the resulting optimization problem is often orders of magnitude faster to solve compared to MCMC approaches.

Scaling VI to large astronomical datasets is nonetheless challenging. The largest published applications of VI have been to text mining, where topic models are fit to several gigabytes of text [9]. The SDSS dataset is four orders of magnitude larger than that. Moreover, most models learned by variational inference to date have a form that allows optimization by coordinate ascent, where each update can be computed without explicitly forming gradients. The Celeste model does not have this property. Our new scalable version of Celeste instead bases its optimization on a variant of Newton’s method, with manually computed gradients and Hessians—a considerably more involved undertaking.

Furthermore, the datasets for topic modeling, and for many machine learning tasks, are modeled as N conditionally independent observations given a modest number of global parameters. Astronomical images, on the other hand, overlap. Light sources are often imaged many times: Figure 1 shows image boundaries for SDSS data. Images have substantial overlap, and even non-overlapping parts of different images receive light from a single light source. The Celeste statistical model accounts for all of these unique characteristics.

III. CELESTE

Celeste approximates the posterior distribution using a variational inference procedure that facilitates parallel processing. The Celeste model and the variational objective function are described in earlier work about a single-threaded version of Celeste [5]. Our approach to optimizing the objective function, based on a trust-region Newton’s method, is new, as is the approach to parallelism.

A. The Celeste Model

A generative Bayesian model is a joint probability distribution over observed random variables (the pixel intensities) and unobserved, or latent, random variables (the catalog entries). The Celeste model is represented graphically in Figure 2.

Images: Each of N images has fixed metadata Λ_n , describing its sky location and the atmospheric conditions at the time of the exposure. Each image contains M pixels. Each pixel intensity is an observed random variable, denoted x_{nm} , that follows a Poisson distribution with a rate parameter F_{nm} unique to that pixel. F_{nm} is a deterministic function of the catalog (which includes random quantities)

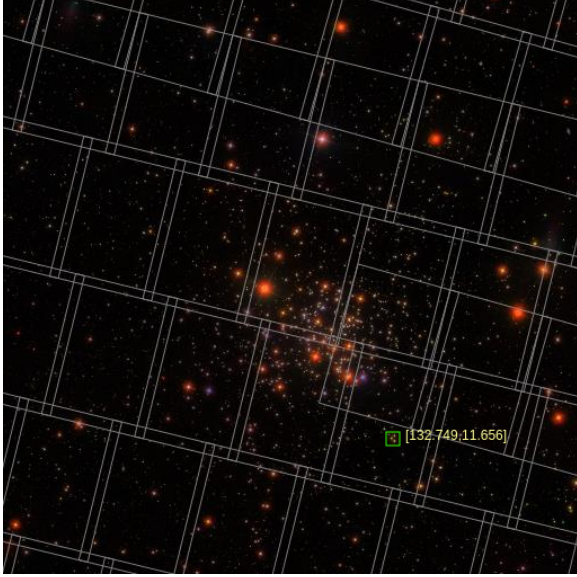


Figure 1: SDSS image boundaries. Some images overlap substantially. Some light sources appear in multiple images that do not overlap. Celeste uses all relevant data to locate and characterize each light source whereas heuristics typically ignore all but one image in regions with overlap. credit: SDSS DR10 Sky Navigate Tool.

and the image metadata. It follows that pixel intensities are conditionally independent given the catalog.

Light sources: For each of S light sources, a Bernoulli random variable a_s indicates whether it is a star or a galaxy; a lognormal random variable r_s denotes its brightness in a particular band of emissions (the “reference band”); and a multivariate normal random vector represents its colors—defined formally as the log ratio of brightnesses in adjacent bands, but corresponding to the colloquial definition of color. These random quantities have prior distributions with parameters Φ , Υ , and Ξ , respectively. These parameters are learned from pre-existing astronomical catalogs. Additionally, each light source is characterized by (non-random) vectors μ_s and φ_s . The former indicates the light source’s location and the latter, if the light source is a galaxy, represents its shape, scale, and morphology. Though non-random, these vectors are nonetheless learned within our inference procedure.

It is straightforward to sample collections of “synthetic” astronomical images from the Celeste model, given the preceding description. Indeed, we do generate data in this way for testing purposes. Our primary use for the model, however, is to compute the distribution of its unobserved random variables conditional on a particular collection of (real) astronomical images. This distribution is known as the posterior. Exact posterior inference is computationally intractable for the Celeste model, as it is for most non-trivial Bayesian models. Instead, we use variational inference to

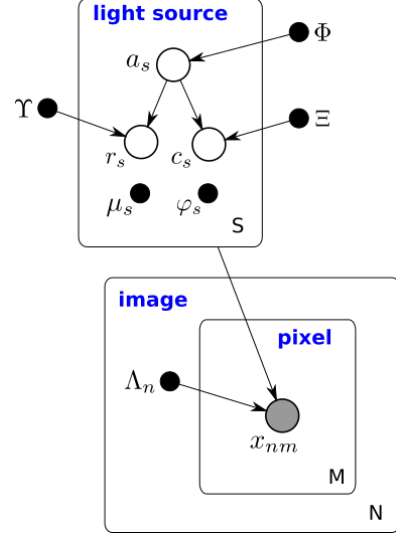


Figure 2: The Celeste graphical model. Shaded vertices represent observed random variables. Empty vertices represent latent random variables. Black dots represent constants. Constants denoted by uppercase Greek characters are fixed throughout our procedure. Constants denoted by lowercase Greek letters are inferred, along with the posterior distribution of the latent random variables. Edges signify permitted conditional dependencies. Plates (the boxes) represent independent replication.

approximate the posterior.

B. Variational Inference

Let $x := \{x_{nm}\}_{n=1, m=1}^{N, M}$ denote all pixels. Let $z := \{a_s, r_s, c_s\}_{s=1}^S$ denote all the latent random variables. The posterior distribution on z , i.e. $p(z|x)$, combines our prior knowledge with the new information contained in the data.

Variational inference (VI) chooses a distribution q from a class of candidates to approximate the posterior $p(z|x)$ by maximizing the following lower bound on the log probability of the data [8]:

$$\log p(x_{11}, \dots, x_{NM}) \geq \mathbb{E}_q [\log p(x, z) - \log q(z)] \quad (1)$$

$$=: \mathcal{L}(\theta). \quad (2)$$

This lower bound holds for every q , which follows from Jensen’s inequality.

We take the density q to factorize across light sources and across each light source’s latent variables:

$$q(z) = \prod_{s=1}^S q(r_s|a_s)q(c_s|a_s)q(a_s). \quad (3)$$

In our formulation, each factor of q is an exponential family that is conjugate to the corresponding prior distribution: $q(r_s|a_s)$ is univariate lognormal, $q(c_s|a_s)$ is multivariate normal, and $q(a_s)$ is Bernoulli.

We index the class of candidate q 's by the real-valued vector θ . Then, maximizing over q is equivalent to maximizing over θ . It can be shown that the maximizer of \mathcal{L} also minimizes

$$D_{\text{KL}}(q(z), p(z|x)), \quad (4)$$

the Kullback-Leibler divergence to the posterior [8]. The objective function \mathcal{L} may also be maximized over the model parameters $\{\mu_s, \varphi_s\}_{s=1}^S$, simultaneously, to estimate them.

The posterior distribution typically will not have the form of the candidate variational distributions, so the minimum Kullback-Leibler divergence will not be zero, and the posterior distribution will not be recovered exactly. For classes of variational distributions that factorize, such as ours, the variational distribution that minimizes Kullback-Leibler divergence tends to underestimate the posterior's variance. Techniques exist to correct this bias [10].

Though q factorizes across the light sources, the light sources are still coupled in \mathcal{L} by $p(x, z)$: pixels may receive photons from multiple light sources. The parameter vector θ contains 32 entries per light source, for each of hundreds of millions of light sources.

To simplify optimization, rather than maximizing \mathcal{L} with respect to all of θ jointly, we optimize subsets of θ corresponding to the parameters for distinct light sources independently, while holding the parameters for other light sources fixed at estimates from previous astronomical surveys. For light sources that do not overlap with any other light sources, the optimal point returned by this technique is no different than had we optimized θ jointly across all light sources. For light sources that do overlap with others, we anticipate that existing estimates of neighboring light sources will be sufficiently accurate. Regardless, $\max_{\theta} \mathcal{L}$ is a lower bound on the log probability of the data. Our alternative optimization procedure may find a looser lower bound, but with significant computational savings from decoupling optimization of the light sources.

In [5], we used L-BFGS [11] to optimize \mathcal{L} . However, some light sources require thousands of L-BFGS iterations to converge. These light sources dominate runtime. The approach based on L-BFGS is too inefficient for large-scale optimization.

For our scalable version of Celeste, we use Newton's method, with updates constrained by a trust region, to optimize \mathcal{L} for each source. Newton's method consistently reaches machine tolerance within 50 iterations for our optimization problems. Furthermore, to maximize efficiency, rather than using automatic differentiation, we manually compute the gradient and the (dense) Hessian for each light source.

C. Parallel Work Decomposition

To find the optimal parameters for a light source, Celeste must load the following: (a) all the images containing that

light source, (b) an initial estimate of its parameters, and (c) initial estimates of any nearby light source that may overlap with it.

Image data is at least an order of magnitude larger than the initial parameter estimates. An image is stored as a collection of five files that are roughly 60 MB in aggregate. Approximately 500 light sources appear in each image. We aim to limit the I/O cost associated with loading images repeatedly.

On a fast, modern processor, Celeste finds the optimal parameters for a light source in anywhere from one second to over two minutes, with most sources taking less than five seconds. Because the work is irregular, we use dynamic scheduling to balance load.

These two aims present a challenge. We must limit I/O—multiple processes loading the same image repeatedly, once for each light source in it, would lead to a severe I/O bottleneck. Yet we cannot distribute work at the image level, as that could lead to load imbalance on the order of minutes.

We considered two work decomposition strategies. The first strategy partitions the sky into equal-size contiguous regions smaller than an image. Each region corresponds to a task. If an image contains R such regions, then at most R nodes must load the same image, limiting the I/O burden. However, our experiments with this approach still showed high load imbalance. Although cosmological theory predicts a certain type of uniformity of light sources across the Universe, in practice we find that some regions of the sky have many sources while other regions have few to none.

For our second strategy, candidate light sources correspond to tasks. Given an existing catalog of light sources, we dynamically schedule batches of light sources to nodes for optimization. Since each image typically contains many light sources, this second strategy could potentially require the same image to be loaded many times by different processes. We use two techniques to reduce the I/O burden: first, we load all images from disk into the memory of all the participating processes, using a global array implementation, thus converting a slow, disk-bound operation into a much faster one-sided RMA operation on a high-performance interconnect fabric. Second, we use a task scheduling scheme that distributes tasks in spatially aware batches, thereby reducing the frequency of multiple processes requiring the same image data.

We implement the second strategy for our experiments.

D. Implementation

The current implementation proceeds in three phases:

1. *Load images*: All required images are loaded into a global array. Each process loads images concurrently, using only a single thread since this stage is I/O bound.

2. *Load catalog*: An existing catalog of candidate light sources is loaded into a second global array. Each entry includes initial estimates of the suspected light sources'

parameters (recall that these initial estimates are used for rendering neighboring light sources during optimization). The candidate light sources are ordered according to their spatial position, thus nearby light sources are also close together in the global array. This ordering reduces communication but is not necessary for correctness.

3. *Optimize sources*: Each entry in the catalog global array is a task. We use the Dtree scheduler [12] to distribute batches of contiguous indices into the catalog global array, to processes. The batches are small to help balance load.

A process uses multiple threads to optimize the light source in the region it is assigned. These threads share a process-level cache of images and catalog entries. Each thread retrieves the next index from the batch assigned to the process, fetches that entry from the catalog global array, and then checks the cache for the necessary images and neighbor catalog entries, fetching them from the global arrays as needed.

E. Language considerations

Celeste is implemented entirely in Julia, a high level dynamic programming language. Julia offers many desirable features for scientists and engineers—familiar syntax, interactive development, a high level of abstraction, garbage collection, dynamic types, and excellent integrated open-source libraries for many areas, including linear algebra and signal processing. Julia’s compiler is based on LLVM. It uses type inference, JIT compilation, vectorization, and inlining to achieve excellent performance, competitive with statically-typed languages such as C/C++.

This combination of features—expressiveness and ease of use, together with high performance—makes Julia a compelling choice for scientific and numerical computing. While still at an early stage with version 0.5 (as of October 2016), the Julia language is maturing rapidly. As such, using Julia presents advantages as well as challenges, particularly relating to parallelism. We discuss these challenges in Section VIII.

F. Multi-process scaling

Julia offers distributed parallelism capabilities in its base libraries. This functionality is built around remote procedure calls (RPC), an abstraction that has limited application to HPC applications, which tend to be mostly data parallel, and have stringent latency and bandwidth needs.

Julia applications can directly use MPI via a wrapper package. However, MPI does not offer high-level abstractions that are easy to use and expressive. The PGAS model [13], on the other hand, was developed precisely to improve the productivity of distributed parallel programming.

Thus, we have developed a lean and fast global arrays library that implements essential parts of the Global Arrays interface [14]. We use MPI-3 as the transport layer for our

library; get and put operations on global array elements make use of one-sided RMA operations that are supported in hardware on most supercomputer fabrics [15]. We have also developed a Julia wrapper package for this library, making the PGAS programming model available to Julia applications such as Celeste.

G. Distributed dynamic scheduling

To serve the dynamic scheduling needs of Celeste, we have written a Julia wrapper for Dtree [12], a distributed dynamic scheduler that has been shown to be capable of balancing load for a diverse range of irregular tasks, even at petascale. The effectiveness of this scheduler can be seen in the minimal scheduling overhead we observed in our experiments.

Dtree organizes processes into a short tree for task distribution; the tree fan-out is configurable and allows for multiple parents in order to eliminate any bottleneck arising from too many children sharing a single parent. Given a total number of tasks, T , parents in the tree distribute batches of number ranges, $f-l$, where $f, l \leq T$ in response to requests from child processes. The size of each batch, $n = l - f$, reduces as T is approached; this balances load.

Celeste uses the size of the catalog global array, that is, the number of candidate light sources, as the total number of tasks, T , as previously described.

IV. SDSS DATASET

The Sloan Digital Sky Survey (SDSS) [16] is the archetypal modern astronomical imaging survey. SDSS Data Release 12 (DR12) contains almost half a billion individual sources. It covers 14,555 square degrees of the night sky. The images are composed of 938,046 “fields”. Each field has images of it stored in five different files, one per filter band. Each file stores one image in the FITS file format. The images are 1361×2048 pixels, and roughly 12 MB each. The dataset in total is 55 TB; we processed 250 GB during the tests reported in this paper.

V. HARDWARE PLATFORM

Our experiments are conducted on the Cori supercomputer at the National Energy Research Scientific Computing Center (NERSC). Cori is a Cray XC40 supercomputer. We used Cori Phase I (also known as the “Cori Data Partition”) which has 1,630 compute nodes, each containing two Intel® Xeon® E5-2698v3 processors¹ (16 cores each) running at 2.3 GHz, and 128 GB of DDR4 memory. Nodes are linked through a Cray Aries high speed “dragonfly” topology interconnect. Datasets used in these experiments were staged on Cori’s 30 PB Lustre file system, which has an aggregate bandwidth exceeding 700 GB/s.

¹Intel, Xeon, and Intel Xeon Phi are trademarks of Intel Corporation in the U.S. and/or other countries.

VI. SCALING RESULTS

We ran a variety of experiments to explore the scalability of Celeste using the parallelization strategy described in Section III-C.

We analyze Celeste’s performance by partitioning the measured runtime for a job into a number of components: (a) garbage collection time, (b) image load time, (c) load imbalance, (d) the time taken in retrieving elements of the global arrays used, (e) dynamic scheduling overhead, and (f) source optimization time. This partitioning is not precise as it is averaged across nodes and certain components of runtime are not completely independent. Nonetheless, it is indicative.

We use a *light-sources-per-second* metric to detail source optimization performance in each scaling test.

A. Single node, multi-threaded performance

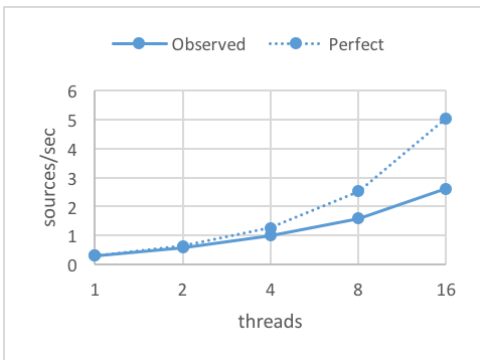


Figure 3: Multi-threaded performance. Strong-scaling Celeste on 154 light sources over up to 16 threads on a Cori Phase I node. Observe that scalability drops off beyond 4 threads; this is due to serial garbage collection.

A Celeste process uses multiple threads to process multiple light sources in parallel. We partition runtime as previously described, and show the number of sources optimized per second at different thread counts in Figure 3. Note the drop-off in scalability beyond 4 threads; this is caused by the serial operation of Julia’s garbage collector, requiring threads to synchronize each GC cycle. Thus, Amdahl’s Law [17] limits multi-threaded scalability. We discuss this challenge further in Section VIII-A.

Software and workloads used in performance tests may have been optimized for performance only on Intel microprocessors. Performance tests, such as SYSmark and MobileMark, are measured using specific computer systems, components, software, operations and functions. Any change to any of those factors may cause the results to vary. You should consult other information and performance tests to assist you in fully evaluating your contemplated purchases, including the performance of that product when combined with other products. For more information go to <http://www.intel.com/performance>.

To limit time in GC, we use 4 threads per process on our multi-node runs. A single Cori Phase I node has 32 cores; we run 8 processes per node.

B. Weak scaling

Figure 4 shows the components of runtime for our weak scaling experiment. Garbage collection takes between 15% and 25% of runtime at all scales. Image load time does not exceed 1% of runtime.

Load imbalance is 6.5% of runtime at most. In absolute terms, 256 nodes exhibits the highest average load imbalance, yet the runtime attributed to load imbalance is less than 70 seconds. This is an acceptable level of imbalance: some individual tasks alone take more than double this time.

The portion of runtime spent retrieving data from the global array is the most concerning. Retrieval time is negligible at 64 nodes and fewer, but grows to 18% of runtime at 256 nodes. Such a growth rate indicates that transferring images between nodes is saturating the fabric bandwidth.

Recall from Section III-C, that Celeste faces a trade-off between I/O burden and load balance. The use of global arrays is intended to reduce the I/O burden, but although the network is far faster than disk, there are nonetheless bandwidth limitations.

Each image is roughly 120 MB in size, and the average task execution time is less than 5 seconds. If every thread in every process executes a task that requires a different image, then every 5 seconds on average, a node will fetch 3.75 GB of image data from across the fabric. Clearly, as the node count increases, even a high performance fabric such as Cray’s Aries HSN would be overwhelmed—for this worst case at 256 nodes, 192 GB of images would have to move across the fabric every second.

These results indicate that we have not sufficiently reduced the I/O burden, however further reduction in I/O will cause increased load imbalance. We will pursue more advanced strategies in future work.

We note the slight increase in scheduling overhead on the 256 node run; this is due to global arrays traffic saturating the interconnect and slowing down the task scheduler, rather than to any issue with the scheduler itself.

Figure 6a shows the light-sources-per-second rate achieved at different scales in the weak-scaling experiments. We observe perfect scaling up to 64 nodes followed by a degradation primarily due to slower fetches from the images global array.

C. Strong scaling

Our strong scaling experiments process a region of the sky containing 332,631 light sources. Figure 5 shows the runtimes, and their breakdowns by routine, at each scale.

Garbage collection time is highest (30% of total runtime) for the 16 node run, the run with the fewest nodes. That indicates that Julia’s serial GC is detrimental not only

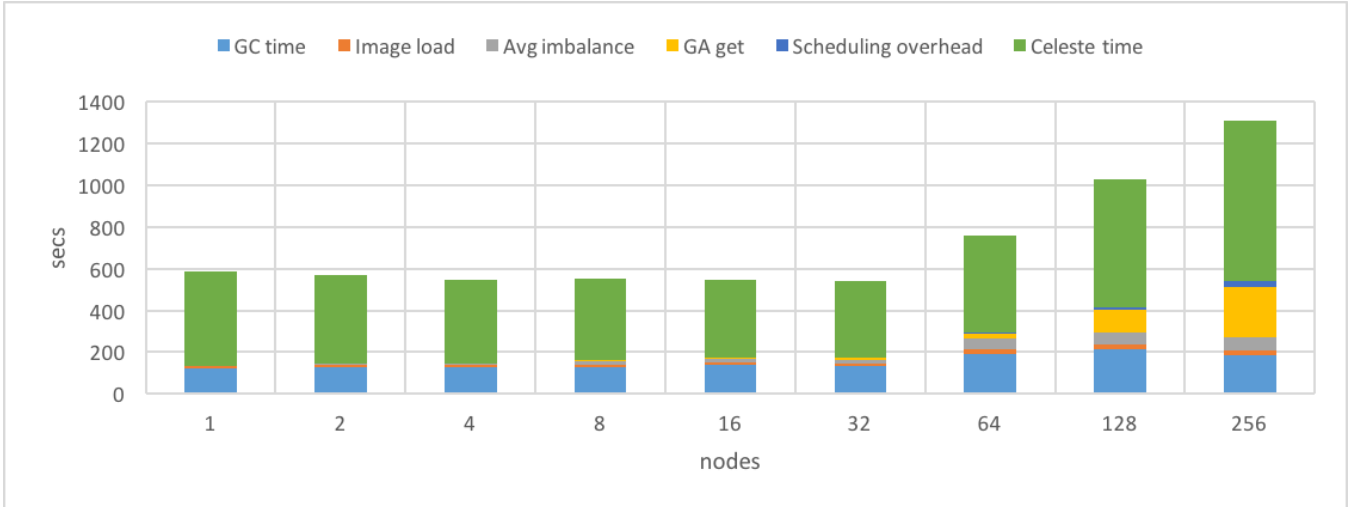


Figure 4: Weak-scaling Celeste. While the total runtime shown is precise, the components of runtime shown are averaged across nodes and thus should be treated as being representative rather than exact.

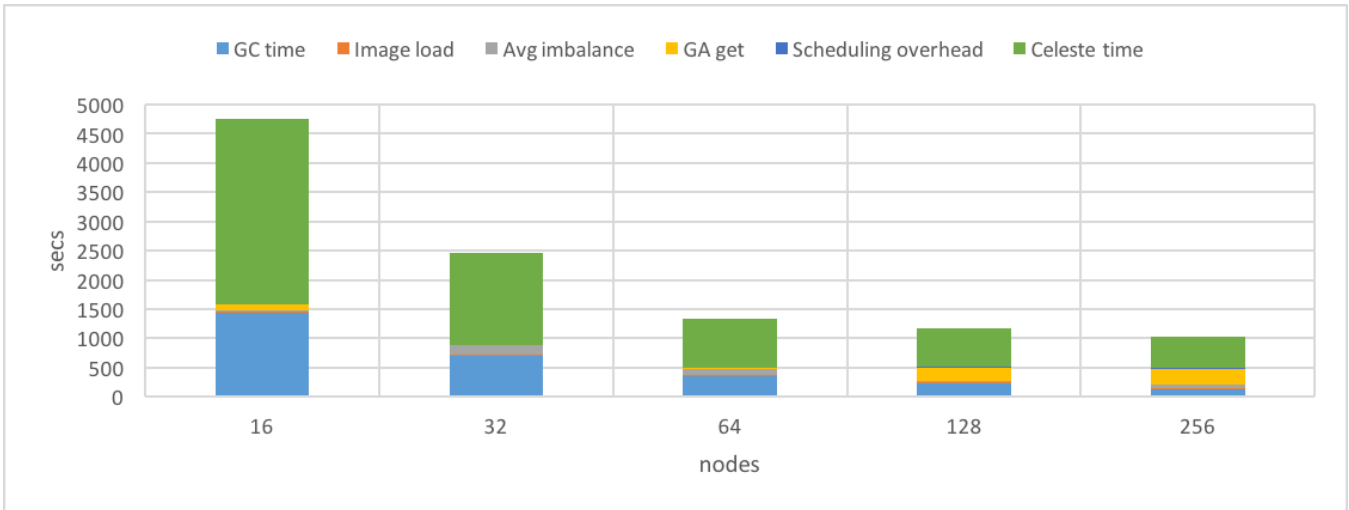


Figure 5: Strong-scaling Celeste. Note the reduction in GC time correlates with reduction in runtime, whereas the increase in global arrays fetch time correlates with the increase in nodes.

for large numbers of threads, but also for long running processes. For the 256 node strong-scaling run, garbage collection time is 11% of total runtime.

This finding further underscores the need for improved GC; see Section VIII-A for further discussion.

The next largest portion of total runtime, global arrays retrieval time, does not exceed 2% of runtime at 16 nodes. However, at 256 nodes, we find that it reaches 26% of runtime, reaffirming the need for improvements in task scheduling to reduce the I/O burden.

The light-sources-per-second rates achieved at different scales in the strong-scaling experiment are shown in Figure 6b. Again, we see perfect scaling up to 64 nodes, followed by a drop-off due to serial GC and fabric bandwidth

saturation.

VII. DISCUSSION: SCIENTIFIC RESULTS

For astronomical images, ground truth is unknowable. That in part is what makes Bayesian models of the data desirable for astronomy: if their output follows a plausible model of the data, then it too is plausible. Nonetheless, validation is essential: every model entails assumptions about the process that generated the data.

A particular region of the sky, known as Stripe 82, has been imaged everywhere at least 30 times. Most other regions have been imaged just once. With images from so many exposures, galaxies and stars that would be faint and hard to accurately characterize with just one exposure are

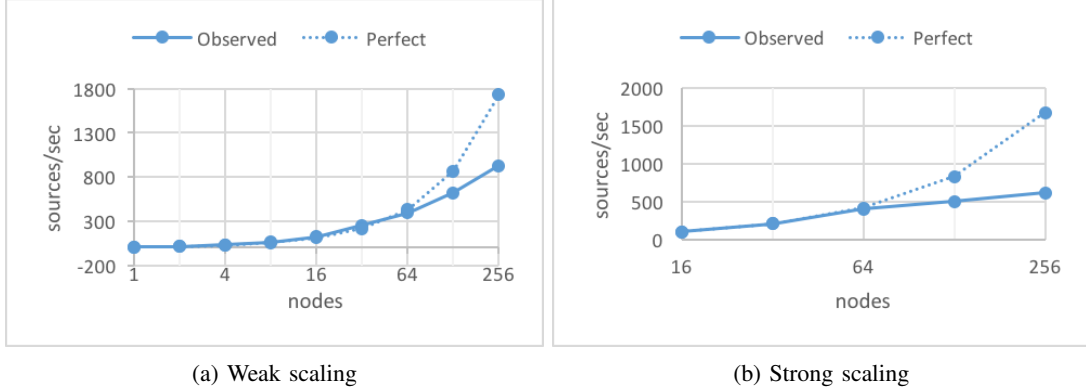


Figure 6: Celeste sources/second. We observe perfect scaling up to 64 nodes, after which we are limited by interconnect bandwidth.

easily resolved.

“Photo” [3] is the current state-of-the-art software pipeline for constructing large astronomical catalogs. Photo is a carefully hand-tuned heuristic. Running Photo on all 30+ exposures of Stripe 82 generates a catalog that we let stand in for ground truth in our subsequent analysis.

The first numeric column of Table I shows average error for Photo itself fit to just one segment of one exposure from Stripe 82. The second numeric column shows average error for Celeste fit to the same data. Celeste has lower error than on Photo by nearly 30% for locating stars and galaxies—an improvement that is both statistically significant and of practical significance to astronomers. For all four colors, Celeste reduces the error rate by large amounts—always at least 30%.

For brightness, Photo outperforms Celeste significantly. That may be due to systematic errors by Photo, reflected in both ground truth as well as Photo’s predictions based on one exposure, but we do not have firm conclusions yet. We have seen cases where a light source is over-saturated, that is, it is too bright for all the photons from it be counted, yet not flagged as being over-saturated. In these cases the ground truth does not reflect reality, but Photo run on all the data largely agrees with itself run on one exposure.

Photo is more likely to misclassify stars as galaxies whereas Celeste is more likely to misclassify galaxies as stars. Photo is more accurate at determining the scales (sizes) of galaxies whereas Celeste is more accurate at determining their eccentricities and angles.

We anticipate that adjustments to the Celeste model, as discussed in Section IX, will enable Celeste to outperform Photo across board. Already, Celeste’s results are the new state-of-the-art by a wide margin for location and color, and thus should be released.

Table I: Average error on celestial bodies from Stripe 82.

	Photo	Celeste
position	0.33	0.24
missed gals	0.06	0.03
missed stars	0.02	0.09
brightness	0.22	0.37
color u-g	1.23	0.69
color g-r	0.40	0.22
color r-i	0.26	0.17
color i-z	0.30	0.13
profile	0.28	0.29
eccentricity	0.19	0.13
scale	1.97	2.79
angle	17.60	12.91

Lower is better. Results in bold are better by more than 2 standard deviations. “Position” is error, in pixels, for the location of the celestial bodies’ centers. “Missed gals” is the proportion of galaxies labeled as stars. “Missed stars” is the proportion of stars labeled as galaxies. “Brightness” measures the reference band (r-band) magnitude. “Colors” are ratios of magnitudes in consecutive bands. “Profile” is a proportion indicating whether a galaxy is de Vaucouleurs or exponential. “Eccentricity” is the ratio between the lengths of a galaxy’s minor and major axes. “Scale” is the effective radius of a galaxy in arcseconds. “Angle” is the orientation of a galaxy in degrees.

VIII. DISCUSSION: JULIA FOR HPC AND BIG DATA ANALYTICS

Developing Celeste in Julia has generally been a positive experience: rapid prototyping, the high level of abstraction, and a rich set of libraries have allowed for high productivity. Julia’s compiler has produced high performance code. Our greatest challenge arose from our use of Julia’s threads, a feature clearly identified as experimental.

A. Threads and garbage collection

Celeste uses Julia’s experimental multi-threading capability for shared memory parallelism. While this capability

is reasonably stable and allows excellent scaling, we discovered an important limitation: Julia’s garbage collector currently does not scale well. With 16 threads per process, the time consumed by garbage collection exceeds a third of total runtime. The GC time approaches half of total runtime for longer duration jobs.

The foremost reason for excessive GC time is that Julia’s garbage collector is serial. Thus, Amdahl’s Law limits scaling. In addition, serial GC requires synchronization of all threads before a collection cycle. Celeste’s work is irregular and threads run mostly asynchronously, which adds additional overhead as compared to applications with regular work such as PDE solvers.

Parallel garbage collection is not a solved problem; there is active research in this area [18]. However, there are a number of well-understood methods to improve scalability, such as parallelizing the marking phase and doing sweeps concurrently with running threads. There are efforts underway to improve Julia’s memory management in these and other ways. Currently, however, to scale beyond 4 to 6 threads requires the programmer to carefully consider memory utilization—avoiding copies and temporaries, and extensively using in-place operations—which hinders the ease and expressiveness of programming in Julia.

Additionally, while Julia’s runtime is thread-safe, much of the standard library currently is not. That too limits the ease of writing multi-threaded programs in Julia.

IX. CONCLUSIONS AND FUTURE WORK

We developed a multi-threaded, distributed version of Celeste, and demonstrated good weak and strong scaling on up to 256 nodes. Using this version of Celeste, we generated a catalog for a subset of SDSS that contains better parameter estimates for location, color, galaxy eccentricity, and galaxy angle. This new catalog is the largest ever to include uncertainty estimates that follow from a realistic model of the data.

In the process of generating the catalog, we scaled Bayesian inference to datasets larger than those reported in the literature, through a combination of mathematical and algorithmic innovations. A widely held view is that Bayesian inference works for small datasets, when accuracy is paramount, but that heuristics are typically necessary. Our results suggest otherwise: given a realistic model, the posterior can be approximated within the available computational budget. Celeste is a unique project that has advanced the frontier of scalable inference methods in the context of a truly large-scale, important scientific application on an advanced HPC architecture.

We have several methodological innovations planned for future work. First, we aim to find a stationary point of our objective function by optimizing all light sources jointly, rather than optimizing each light source with all other light

sources’ parameters fixed to their estimates from previous surveys. That requires greater communication among nodes.

Second, we plan to allow candidate light sources to “turn off”, effectively estimating the true number of light sources from an oversubscribed list of candidates.

Third, we will apply linear response methods [10] to improve the uncertainty quantification of our variational inference procedure. These methods should mitigate bias stemming from our choice of a variational distribution that factorizes and provide us with uncertain estimates for quantities that we model as unknown constants rather than random variables.

Fourth, we anticipate switching from deterministic to stochastic optimization. By basing updates on samples from the variational distribution, stochastic optimization can approximate the posterior for arbitrary combinations of models and classes of candidate variational distributions, whereas deterministic optimization is limited to combinations that lead to an analytic objective function. That frees us to experiment with even more realistic models of the data, and even more expressive distributions for approximating the posterior.

Stochastic optimization, however, is likely to be orders of magnitude more computationally expensive than our current highly optimized form of second-order deterministic optimization. Fortunately, the upcoming integration of Cori Phase II (based on Intel Phi Knights Landing processors) will increase the system’s computational throughput by roughly one order of magnitude. An additional order of magnitude speedup may follow from subsampling the pixels, in addition to sampling from the variational distribution—an approach known as “doubly” stochastic VI [19]. Another order of magnitude speedup may follow from using a second-order stochastic method [20] rather than stochastic gradient descent.

Finally, applying Celeste to multiple images surveys jointly is a promising direction. In conjunction with SDSS, we will process the Dark Energy Camera Legacy Survey (DECaLS) [21] in future work.

ACKNOWLEDGMENTS

This research used resources of the National Energy Research Scientific Computing Center (NERSC), a DOE Office of Science User Facility supported by the Office of Science of the U.S. Department of Energy under Contract No. DE-AC02-05CH11231. The authors express their gratitude to Tina Declerck, Doug Jacobsen, David Paul and Zhengi Zhao who helped make the results presented in this paper possible. Debbie Bard and Dustin Lang provided expert advice on astronomy datasets and image processing issues. We are grateful for the tremendous assistance rendered by various members of the Julia developer community: Tony Kelman, Jameson Nash, Andreas Noack, Alan Edelman and Viral Shah addressed various functionality and performance

issues in Julia. Finally, we thank Andy Miller, Ryan Adams and Steve Howard, who assisted in developing the Celeste codebase.

Funding for the Sloan Digital Sky Survey IV has been provided by the Alfred P. Sloan Foundation, the U.S. Department of Energy Office of Science, and the Participating Institutions. SDSS-IV acknowledges support and resources from the Center for High-Performance Computing at the University of Utah. The SDSS web site is www.sdss.org.

REFERENCES

- [1] Large Synoptic Survey Telescope Consortium, <http://www.lsst.org/lsst/about>, 2016, [Online; accessed October 18, 2016].
- [2] E. Bertin and S. Arnouts, “SExtractor: Software for source extraction,” *Astronomy and Astrophysics Supplement Series*, vol. 117, no. 2, pp. 393–404, 1996.
- [3] R. H. Lupton, Z. Ivezić, J. E. Gunn, G. Knapp, M. A. Strauss, M. Richmond, N. Ellman, H. Newburg, X. Fan, N. Yasuda *et al.*, “SDSS image processing II: The photo pipelines,” Technical report, Princeton University, Tech. Rep., 2005.
- [4] M. D. Schneider, D. W. Hogg, P. J. Marshall, W. A. Dawson, J. Meyers, D. J. Bard, and D. Lang, “Hierarchical probabilistic inference of cosmic shear,” *The Astrophysical Journal*, vol. 807, no. 1, p. 87, 2015.
- [5] J. Regier, A. Miller, J. McAuliffe, R. Adams, M. Hoffman, D. Lang, D. Schlegel, and Prabhat, “Celeste: Variational inference for a generative model of astronomical images,” in *Proceedings of the 32nd International Conference on Machine Learning*, 2015.
- [6] D. Lang, <http://thetractor.org/about/>, 2016, [Online; accessed October 21, 2016].
- [7] B. J. Brewer, D. Foreman-Mackey, and D. W. Hogg, “Probabilistic catalogs for crowded stellar fields,” *The Astronomical Journal*, vol. 146, no. 1, p. 7, 2013.
- [8] D. M. Blei, A. Kucukelbir, and J. D. McAuliffe, “Variational inference: A review for statisticians,” *arXiv preprint arXiv:1601.00670*, 2016.
- [9] M. D. Hoffman, D. M. Blei, C. Wang, and J. W. Paisley, “Stochastic variational inference,” *Journal of Machine Learning Research*, vol. 14, no. 1, pp. 1303–1347, 2013.
- [10] R. J. Giordano, T. Broderick, and M. I. Jordan, “Linear response methods for accurate covariance estimates from mean field variational bayes,” in *Advances in Neural Information Processing Systems*, 2015, pp. 1441–1449.
- [11] S. Wright and J. Nocedal, “Numerical optimization,” *Springer Science*, vol. 35, pp. 67–68, 1999.
- [12] K. Pamnany, S. Misra, V. Md, X. Liu, E. Chow, and S. Aluru, “Dtree: Dynamic task scheduling at petascale,” in *International Conference on High Performance Computing*. Springer, 2015, pp. 122–138.
- [13] Tim Stitt, <http://cnx.org/content/m20649/latest/>, 2016, [Online; accessed October 23, 2016].
- [14] J. Nieplocha, B. Palmer, V. Tipparaju, M. Krishnan, H. Trease, and E. Aprà, “Advances, applications and performance of the global arrays shared memory programming toolkit,” *International Journal of High Performance Computing Applications*, vol. 20, no. 2, pp. 203–231, 2006.
- [15] T. Hoefler, J. Dinan, R. Thakur, B. Barrett, P. Balaji, W. Gropp, and K. Underwood, “Remote memory access programming in mpi-3,” *ACM Trans. Parallel Comput.*, vol. 2, no. 2, pp. 9:1–9:26, Jun. 2015. [Online]. Available: <http://doi.acm.org/10.1145/2780584>
- [16] C. Stoughton, R. H. Lupton, M. Bernardi, M. R. Blanton, S. Burles, F. J. Castander, A. Connolly, D. J. Eisenstein, J. A. Frieman, G. Hennessy *et al.*, “Sloan digital sky survey: early data release,” *The Astronomical Journal*, vol. 123, no. 1, p. 485, 2002.
- [17] M. D. Hill and M. R. Marty, “Amdahl’s law in the multicore era,” *IEEE Computer*, vol. 41, pp. 33–38, 2008.
- [18] R. Jones, A. Hosking, and E. Moss, *The Garbage Collection Handbook: The Art of Automatic Memory Management*, 1st ed. Chapman & Hall/CRC, 2011.
- [19] M. Titsias and M. Lázaro-Gredilla, “Doubly stochastic variational bayes for non-conjugate inference,” in *Proceedings of The 31st International Conference on Machine Learning*, 2014, pp. 1971–1979.
- [20] J. Blanchet, C. Cartis, M. Menickelly, and K. Scheinberg, “Convergence rate analysis of a stochastic trust region method for nonconvex optimization,” *arXiv preprint arXiv:1609.07428*, 2016.
- [21] Dark Energy Camera Legacy Survey (DECaLS), <http://legacysurvey.org/decamls/>, 2016, [Online; accessed October 20, 2016].